Amphipolar Core−Shell Cylindrical Brushes as Templates for the Formation of Gold Clusters and Nanowires

Ramin Djalali, Shu-You Li, and Manfred Schmidt*

Institut für Physikalische Chemie, Universität Mainz, Jakob-Welder-Weg 11, D-55099 Mainz, Germany

Received July 31, 2001; Revised Manuscript Received January 28, 2002

ABSTRACT: Methacryloyl end-functionalized block copolymers consisting of styrene and vinyl-2-pyridine were polymerized to poly(block co-macromonomer)s with a much higher main chain than side chain degree of polymerization. Like homo-polymacromonomers these molecules exhibit the structure of cylindrical brushes. Since the vinylpyridine block is coupled to the polymerizable group, the resulting cylindrical macromolecules exhibit a core of vinylpyridine and a shell of polystyrene, thus forming an amphipolar core−shell cylindrical macromolecule. The core−shell character of the molecules was demonstrated by HRTEM utilizing selective positive staining for the core and for the core and the shell. The core of the cylindrical brushes was loaded with $HAuCl_4$ in toluene or methylene chloride followed by reduction of the noble metal salt by the electron beam, by UV light, or by chemical reducing agents. Depending on the amount of complexed noble metal ions and the reduction conditions, either a linear array of noble metal cluster or a continuous nanowire is formed most probably within the core of the cylindrical brushes. The resulting metal nanowires are much longer than the individual core−shell macromolecules which is caused by a yet unexplained specific end-to-end aggregation of the cylindrical polymers upon loading with $HAuCl_4$.

Introduction

In recent years, an overwhelming number of papers dealing with the formation of nanowires or ordered arrays of metal and semiconductor clusters have been published.[1−11] Electrochemical reduction under various conditions was successfully utilized to prepare gold nanorods with aspect ratios up to 4 or single-crystal copper rods with 25 nm diameter,[12] the most impressive success so far. Metal clusters or stable nanoclusters were organized in Al_2O_3 pores to form one-dimensional arrays.[13−15] Frequently, rodlike templates like DNA[16] or carbon nanotubes[17] were decorated with densely packed gold clusters. Subsequent annealing yielded continuous metal structures with somewhat irregular shapes and pronounced multicrystalline boundaries.

Polymacromonomers with a much larger main chain than side chain degree of polymerization are shown to exhibit the form of cylindrical brush polymers. The side chains may be linear[18−27] or dendritically branched[28−32] and may exhibit a block structure,[33−36] leading to amphipolar core−shell cylindrical brushes.

We here utilize core−shell cylindrical brushes for the synthesis of metal clusters and wires within such a macromolecular template. The characterization of the resulting structures is performed by atomic force microscopy (AFM) and high-resolution transmission electron microscopy (HRTEM).

Experimental Section

Synthesis. Amphipolar core−shell cylindrical brushes with a vinylpyridine core and a polystyrene shell were prepared by polymerization of a block co-macromonomer consisting of 9 vinylpyridine and 27 styrene repeating units (M_n = 3727 g/mol, according to MALDI-TOF) as described elsewhere.[33] For the preparation of gold clusters the amphipolar cylindrical brushes were dissolved in toluene or methylene chloride, and an excess of $HAuCl_4$ crystals were added. After about 4 days the

Scheme 1. Illustration of the Concept for Nanowire Formation[a]

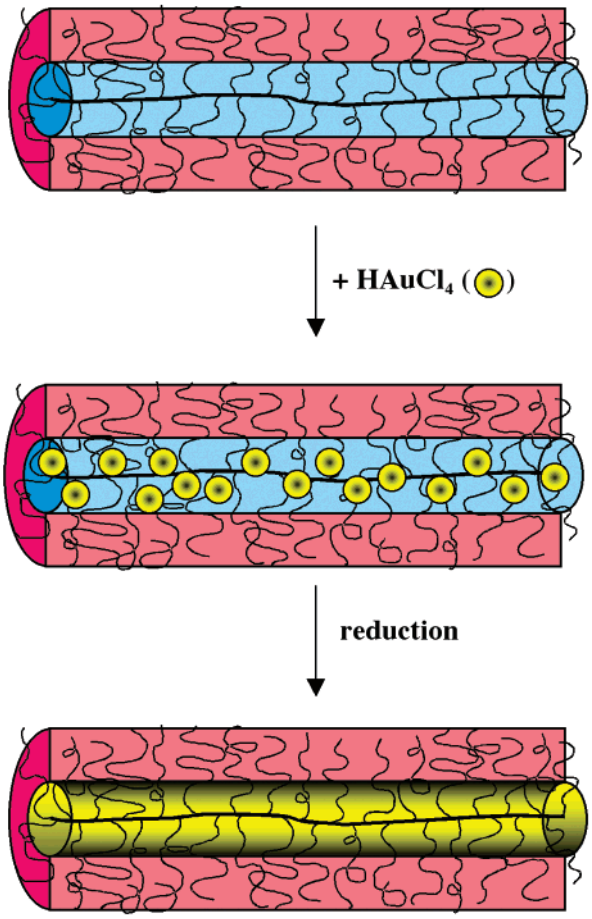

[a] Core−shell cylindrical brushes with a PVP core (blue) and PS shell (red) are loaded with $HAuCl_4$ (Yellow ○). Subsequent reduction yields a one-dimensional gold phase (yellow) within the macromolecular brush.

10.1021/ma0113733 CCC: $22.00
Published on Web 04/20/2002

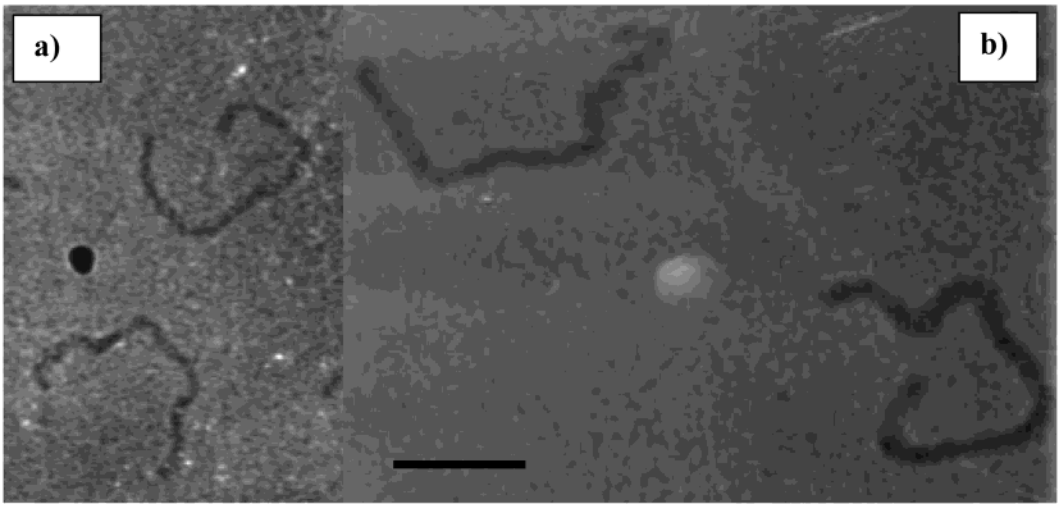

Figure 1. TEM micrographs of the poly(block co-macromonomer): (a) core stained with tetrachloroauric acid; (b) additional staining with ruthenium tetraoxide vapor. The observed diameter increases from 6 nm (a) to 12 nm (b). Scale bar indicates 60 nm.

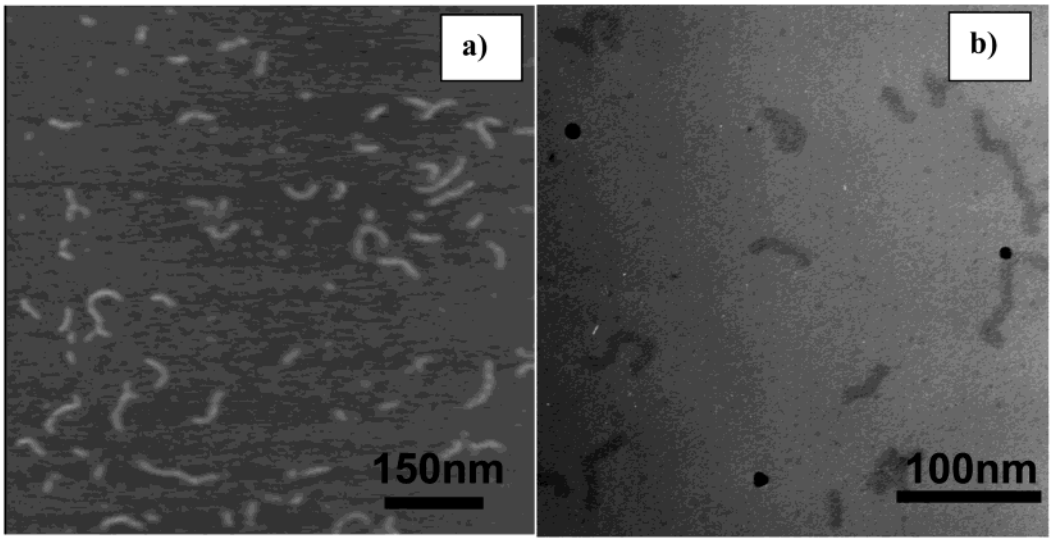

Figure 2. AFM (a) and TEM (b) images of poly(block co-macromonomer). For TEM the polymer was stained with ruthenium tetraoxide vapor.

maximum loading of one $HAuCl_4$ molecule per vinylpyridine unit was achieved as determined by UV−vis spectroscopy.

In a first set of experiments the loaded brushes were spin-cast onto carbon grids and reduced by exposure to the electron beam of variable energy. Alternatively, the spin-cast brushes were exposed to UV light for a maximum duration of 36 h. The resulting clusters were characterized by HRTEM and AFM as described below.

Sample Preparation. For electron microscopy, the solution was dropped onto a gold grid coated with carbon and was allowed to dry gradually. For AFM investigations one drop of a 1% solution of polymer in methylene chloride was placed on a freshly cleaved graphite surface and spin-cast for AFM investigations. A thin support film (1% Formvar in chloroform) was prepared on copper grids with numbered meshes (300 lines/in.). Then the grids were coated with carbon and employed for subsequent TEM and AFM investigations.

Instrumentation. Atomic force micrographs were recorded with a Nanoscope III instrument (Digital Instruments, St. Barbara, CA) operating in tapping mode at a resonance frequency of about 280 kHz.[20,21,37] Transmission electron microscopy (TEM) was performed in the dark field mode on a PHILLIPS EM 300 microscope operating at 80 keV and on a PHILLIPS Tecnai F30 ST (300 keV) microscope.

Static and dynamic light scattering was performed with an ALV SP-86 goniometer, an ALV-3000 correlator, and a krypton ion laser (Spectra Physics 2060-11, 647.1 nm, 500 mW) as described elsewhere.[38] Unfortunately, such measurements are not easily performed because intermolecular structure formation due to electrostatic interaction may prohibit an unambiguous interpretation of the data.[39] Therefore, we selected dimethylformamide with lithium bromide salt (10^{-2} mol/L) as the solvent. Polymer concentrations ranged from 0.4 to 0.04 g/L. The refractive index increment of the unloaded polymacromonomer was determined in DMF with salt by a home-built interferometer[40] to $dn/dc = 0.165$ cm^3/g at 632.8 nm wavelength.

Results and Discussion

Poly(block comacromonomer)s consisting of a poly(2-vinylpyridine) and of a polystyrene block with the methacryloyl group attached to the poly(vinylpyridine) end should exhibit the topology of core−shell cylindrical brushes. The main chain and the poly(vinylpyridine) form the core surrounded by a polystyrene corona as shown in Scheme 1. The strategy to create metal structures within the cylindrical brush involves loading of the PVP core with $HAuCl_4$ by protonation and/or complexation followed by reduction of the $[AuCl_4]^-$ ions to elemental gold. The procedure is illustrated in

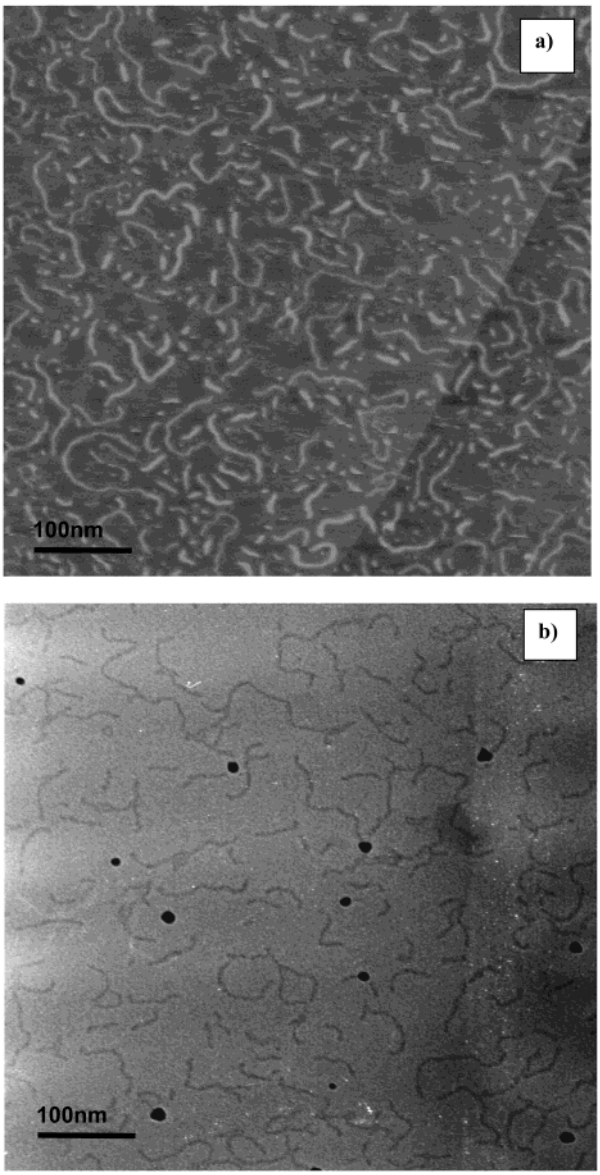

Figure 3. AFM (a) and TEM (b) images of end-to-end aggregated poly(block co-macromonomer) loaded with $HAuCl_4$.

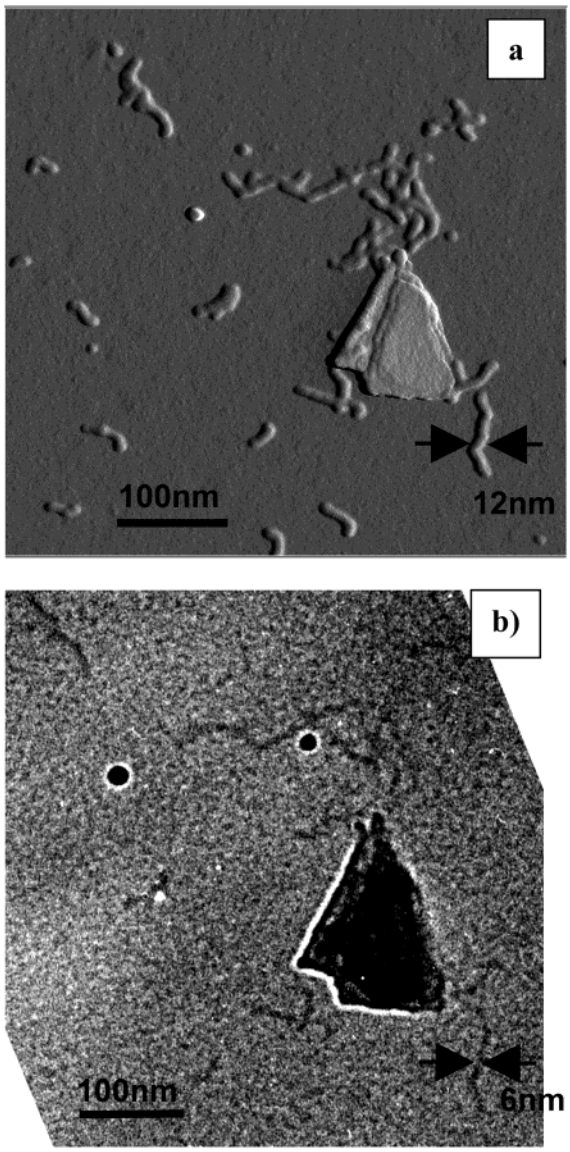

Figure 4. Visualization of identical molecules by AFM (a) and TEM (b).

Scheme 1. Besides proving the core−shell topology, the challenge of the present paper is to achieve a sufficient loading of the core with $HAuCl_4$ in order to produce a continuous gold phase rather than an array of gold clusters.

Core−Shell Topology of the Cylindrical Brushes. To prove the amphipolar core−shell structure of the molecules, we utilized selective positive staining techniques for the core and for both the core and the shell. First, the cylindrical core was loaded with $HAuCl_4$. The contrasted part of the molecules have a diameter of $d = 6$ nm (see Figure 1a) which is attributed to the core dimension of the cylindrical brush. By positive staining of both the PVP core and the PS shell, with RuO_4 a diameter $d = 12$ nm (Figure 1b) is observed. Assuming a circular cross section of the molecules at the surface and the same density for the PVP and the PS phase the core radius and the shell thickness should be equal for the given ratio of vinylpyridine to styrene units (1:3), which is indeed observed. However, the molecules are deformed at the surface, i.e., 12 nm wide and 3 nm high as determined by cross-section analysis of the AFM pictures. Since the precise internal structure of the flattened cylinders is not known, it is difficult to quantitatively interpret the observed diameters in terms of the monomer ratio. However, the core−shell topology of the cylindrical brushes is unambiguously proven.

End-to-End Aggregation of Metal-Loaded Cylindrical Brushes. The cylindrical brushes spin-cast from methylene chloride onto graphite- or carbon-coated TEM grids are visualized by AFM and by TEM as shown in Figure 2a,b. Short cylindrical molecules are observed with number- and weight-average lengths of about $L_n = 38$ nm and $L_w = 72$ nm, respectively. This ought to be compared to the light scattering measurements yielding the weight-average molar mass $M_w = 1\,335\,000$ g/mol, the square root of the *z*-average mean-square radius of gyration $R_g = 29.6$ nm, and the inverse *z*-average of the reciprocal hydrodynamic radius $R_h = 19$ nm. Such values are typical for polydisperse cylindrical brush molecules of considerable chain stiffness. A more quantitative interpretation in terms of chain stiffness is, however, not meaningful for data of one molar mass only. From the degree of polymerization $P_w = 358$, L_w is available if the cylinder length per

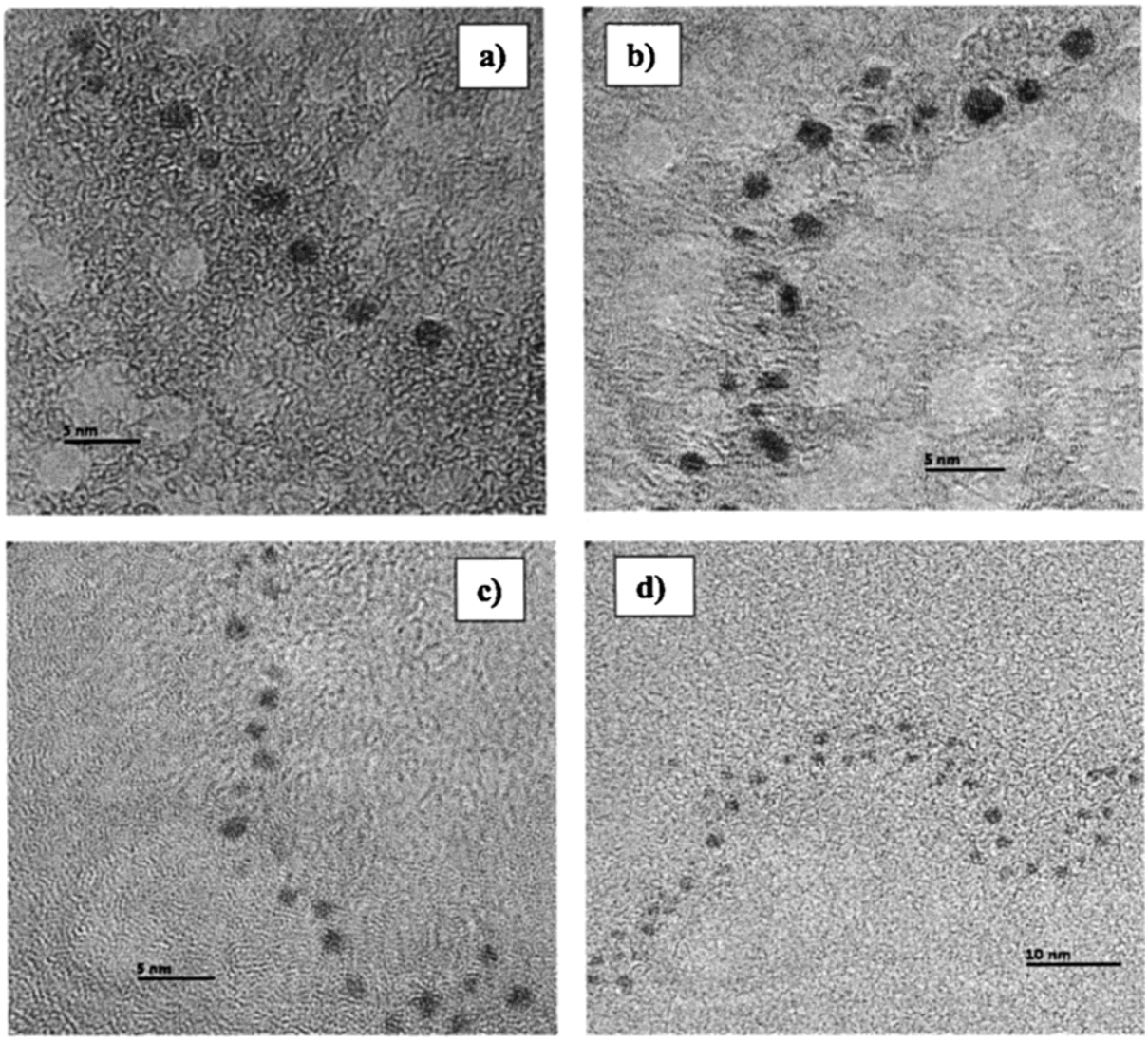

Figure 5. Series of HRTEM images of the gold colloids created by exposure of the $HAuCl_4$-loaded brushes to an electron beam at various energies: (a) 80, (b) 150, (c) 200, and (d) 280 keV.

monomer l is known. From our previous investigations on similar brushes l was found to be always significantly shorter than the maximum contour length of a vinylic main chain monomer $l_{max} = 0.25$ nm. This is also observed for the present poly(block co-macromonomer). Dividing $L_w = 72$ nm as determined by AFM by P_w derived from light scattering, a cylinder length per monomer $l = 0.2$ nm is determined, in qualitative agreement with earlier work.[20,22,41,42] Loading the same sample with $HAuCl_4$ leads to the pictures shown in Figure 3a,b where much longer cylindrical structures are seen. The longer cylinders can only originate from a peculiar end-to-end aggregation, the extent of which depends on subtle variations in concentration, $HAuCl_4$ load, and solvent quality. It should be noted that end-to-end aggregation is also observed if the cylinders were loaded with $CuCl_2$, H_2PtCl_6, $PdAc_2$, and $CoCl_2$.

To ensure that TEM and AFM provide reliable and identical information on the structures being formed, we developed a special sample preparation (see Experimental Section), which allows AFM measurements on a TEM grid. In Figure 4 the AFM (a) and TEM (b) pictures show exactly the same cylindrical polymers. This clearly demonstrates that both techniques are applicable to visualize real polymer structures; i.e., artifacts can be excluded. Because of the very small $HAuCl_4$ load (≈5%) of the cylinders shown in Figure 4, the end-to-end aggregation has not yet occurred to a significant extent.

For higher $HAuCl_4$ loads we obviously face the strange occurrence of a specific end-to-end aggregation, which may occur either in bulk solution or during the adsorption/drying process at the carbon surface. To clarify this point, dynamic light scattering was performed during the loading process of the cylindrical brushes with $HAuCl_4$. The polymer concentration was kept constant at $c = 0.05$ g/L. Besides an increase in scattering intensity, R_g and R_h remained constant upon loading. This proves that the end-to-end aggregation does not occur in dilute solution but rather proceeds during the spin-casting process, i.e., either at much higher concentrations or surface induced. To clarify this question, much more elaborate work is needed which is beyond the scope of the present paper.

Cluster Formation by Electron Beam and UV Light. The formation of gold cluster by exposure of the $HAuCl_4$-loaded brushes to an electron beam was monitored in the Tecnai F30 instrument as a function of electron beam energy. As shown in Figure 5, at small

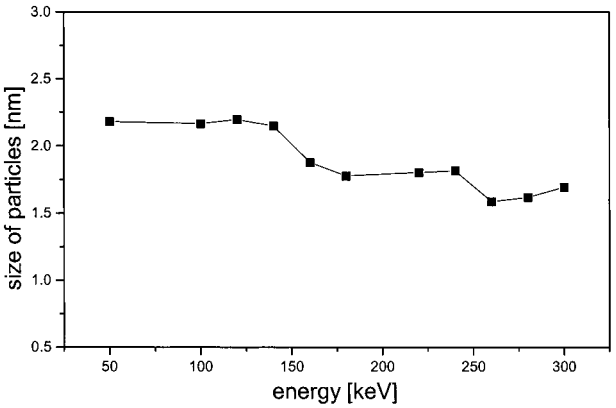

Figure 6. Size of cluster as a function of electron beam energy.

electron beam energies fewer but larger clusters are being formed whereas at high intensities many small clusters were produced. This is qualitatively understood because fewer nucleation sites are being produced at low beam energies which grow to larger clusters due to Ostwald ripening. At high beam energies many small nucleation sites grow simultaneously and become immobilized at a certain size which prohibits further fusion. The cluster sizes as a function of electron beam energies are summarized in Figure 6. The standard deviation of the cluster size ranges typically from $0.2 \leq \sigma \leq 0.3$ nm.

In a second set of experiments the $HAuCl_4$-loaded brushes were exposed to UV light (14 mW/cm^2, 254 nm) in solution for various time intervals. After 2 h exposure many small colloids were formed in a size range of 2 nm (see Figure 7a). After 8 h, 5 nm clusters are observed (Figure 7b) which do not grow upon further exposure up to 72 h (Figure 7c). Obviously, also the end-to-end aggregation is affected by the UV exposure as the aggregate length is seen to steadily increase with increasing exposure duration. After 120 h (Figure 7d) also sidewise aggregation has occurred and has led to very large polydisperse clusters (≈5−50 nm). Eventually precipitation is observed.

Continuous Nanowires. As many successful experiments in science are more or less accidental, we investigated one more $HAuCl_4$-loaded sample by TEM which was exposed to sunlight for 4 days. The TEM pictures show beautiful long nanowires of gold which are several micrometers in length (see Figure 8a). HRTEM shows typical grain boundaries where the growing clusters have fused (Figure 8b). Since this experiment is not easily reproduced, several attempts were made to chemically reduce the $HAuCl_4$-loaded cylinders in solution with hydrazine as the reducing agent. Here, much less defined nanowires were formed

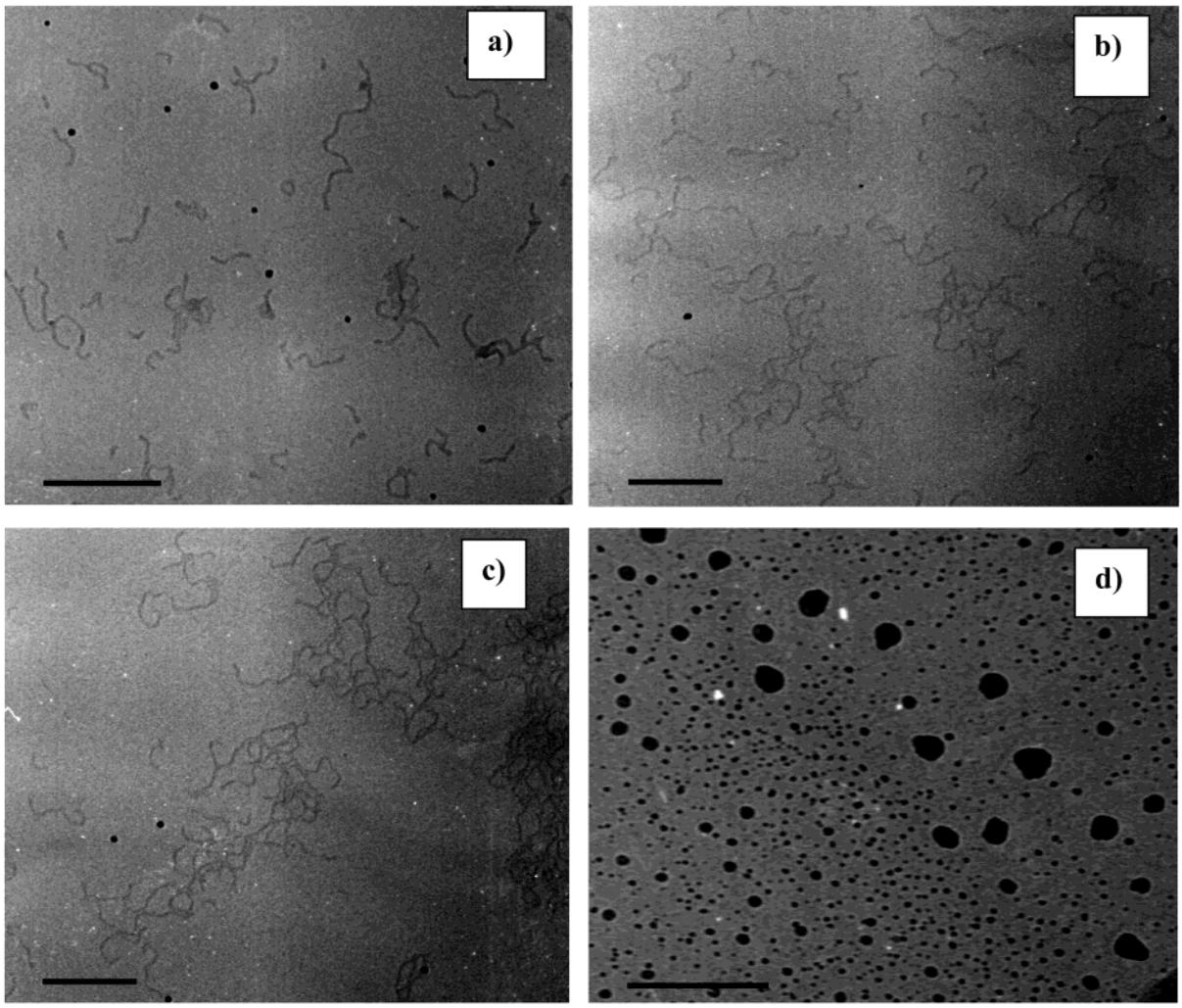

Figure 7. Series of TEM images of $HAuCl_4$–loaded brushes exposed to UV light in solution for various time intervals: (a) 2, (b) 8, (c) 72, and (d) 120 h. Scale bar represents 150 nm.

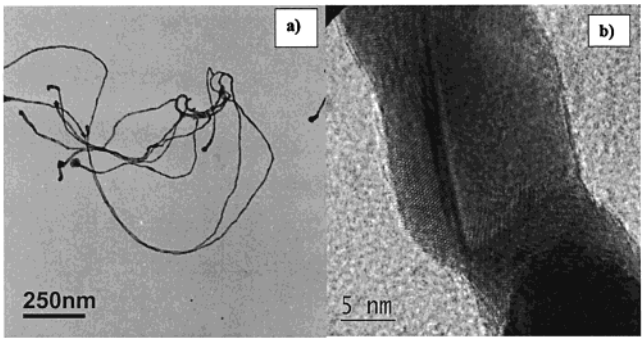

Figure 8. TEM images of gold nanowires with a diameter of 12 nm (a). Magnification by HRTEM shows typical grain boundaries (b).

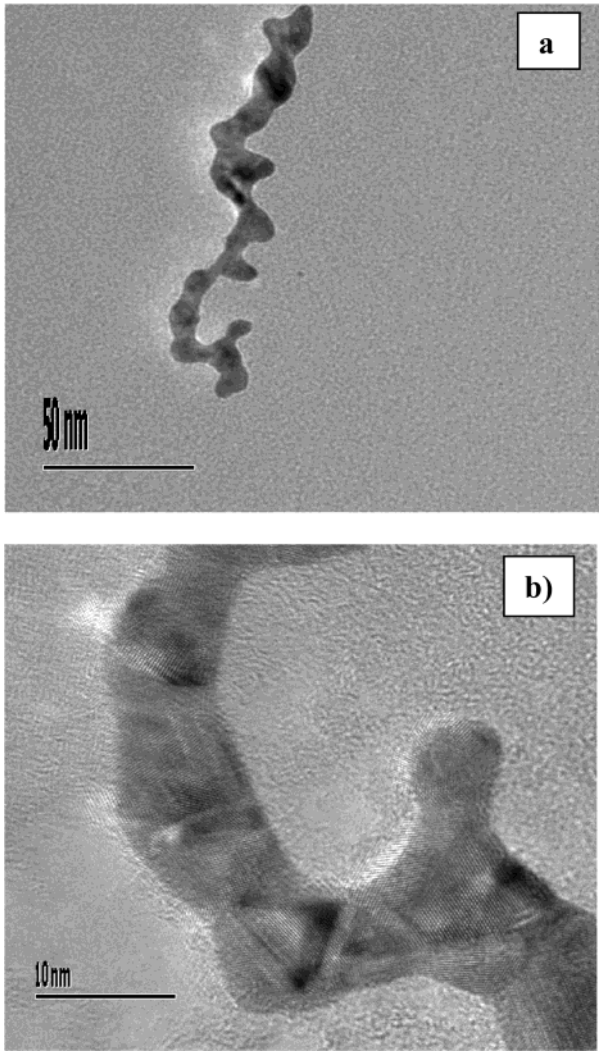

Figure 9. TEM images of gold nanowires prepared by reduction with hydrazine.

with a large variation in thickness (Figure 9a,b). Clearly, the chemical reduction has to be optimized in order to gain control over nanowire formation.

Conclusions

Core−shell nanostructured cylindrical brushes may be utilized as templates for noble metal clusters and nanowire formation. Since the metal formation occurs within the core of the polymer, the shell may serve as the electrically insulating layer. Future work will address conductivity measurements as well as the manipulation of the molecules on nanoscopic length scales.

Acknowledgment. Financial support of the Deutsche Forschungsgemeinschaft, the Fonds der Chemischen Industrie, the Material Science Center of the University of Mainz, and the BMBF-Center for "Multifunctional Materials and Miniaturized Devices" (03N6500) is gratefully acknowledged. We are also indebted to Dr. Dr. I.-G. Voigt-Martin for fruitful discussions.

References and Notes

(1) Govindaraj, A.; Satishkumar, B. C.; Nath, M.; Rao, C. N. R. *Chem. Mater.* **2000**, *12*, 202.
(2) Mohamed, M. B.; Ismail, K. Z.; Link, S.; El-Sayed, M. A. *J. Phys. Chem. B* **1998**, *102*, 9370.
(3) Yu, Y. Y.; Chang, S. S.; Lee, C. L.; Wang, C. R. C. *J. Phys. Chem. B* **1997**, *101*, 6661.
(4) Chen, C. C.; Chao, C. Y.; Lang, Z. H. *Chem. Mater.* **2000**, *12*, 1516.
(5) Han, Y. J.; Kim, J. M.; Stucky, G. D. *Chem. Mater.* **2000**, *12*, 2068.
(6) Liu, S.; Yue, J.; Gedanken, A. *Adv. Mater.* **2001**, *9*, 13.
(7) Molares, M. E. T. V.; Buschmann, D.; Dobrev, R.; Neumann, R.; Scholz, I.; Schuchert, U.; Vetter, J. *Adv. Mater.* **2001**, *1*, 62.
(8) Yonezawa, T.; Onoue, S.; Kimizuka, N. *Adv. Mater.* **2001**, *2*, 140.
(9) Mbindyo, J. K. N.; Reiss, B. D.; Martin, B. R.; Keating, C. D.; Natan, M. J.; Mallouk, T. E. *Adv. Mater.* **2001**, *4*, 249.
(10) Spatz, J. P.; Mossmer, S.; Möller, M.; Herzog, T.; Plettl, A.; Ziemann, P.; Lumin, J. *Adv. Mater.* **1998**, *76*, 168.
(11) Förster, S.; Antonietti, M. *Adv. Mater.* **1998**, *10*, 195.
(12) Lisiecki, I.; Filankembo, A.; Sack-Kongehl, H.; Weiss, K.; Pileni, M. P.; Urban, J. *Phys. Rev. B* **2000**, *61*, 4968.
(13) Benfield, R. E.; Grandjean, D.; Kröll, M.; Pugin, R.; Sawitowski, T.; Schmid, G. *J. Phys. Chem. B* **2001**, *105*, 1961.
(14) Hornyak, G.; Kröll, M.; Pugin, R.; Sawitowski, T.; Schmid, G.; Bovin, J. O.; Karsson, G.; Hofmeister, H.; Hopfe, S. *Chem. Eur. J.* **1997**, *3*, 1951.
(15) Hanaoka, T. A.; Heilmann, A.; Kröll, M.; Kormann, H. P.; Sawitowski, T.; Schmid, G.; Jutzi, P.; Klipp, A.; Kreibig, U.; Neuendorf, R. *Appl. Organomet. Chem.* **1998**, *12*, 367.
(16) Braun, E.; Eichen, Y.; Sivan, U.; Ben-Yoseph, G. *Nature (London)* **1998**, *391*, 775.
(17) Fullam, S.; Cottell, D.; Rensmo, H.; Fitzmaurice, D. *Adv. Mater.* **2000**, *19*, 1430.
(18) Wintermantel, M.; Schmidt, M.; Tsukahara, Y.; Kajiwara, K.; Kohjiya, S. *Macromol. Rapid Commun.* **1994**, *15*, 279.
(19) Wintermantel, M.; Gerle, M.; Fischer, K.; Schmidt, M.; Wataoka, I.; Urakawa, H.; Kajiwara, K.; Tsukahara, Y. *Macromolecules* **1996**, *29*, 978.
(20) Dziezok, P.; Sheiko, S. S.; Fischer, K.; Schmidt, M.; Möller, M. *Angew. Chem.* **1997**, *109*, 2894.
(21) Sheiko, S. S.; Gerle, M.; Fischer, K.; Schmidt, M.; Möller, M. *Langmuir* **1997**, *13*, 5368.
(22) Gerle, M.; Fischer, K.; Roos, S.; Müller, A. H. E.; Schmidt, M.; Sheiko, S. S.; Prokhorova, S.; Möller, M. *Macromolecules* **1999**, *32*, 2629.
(23) Ito, K.; Kawaguchi, S. *Adv. Polym. Sci.* **1999**, *142*, 129.
(24) Furuhashi, H.; Kawaguchi, S.; Itsuno, S.; Ito, K. *Colloid Polym. Sci.* **1997**, *275*, 227.
(25) Deffieux, A.; Schappacher, M. *Macromolecules* **1999**, *32*, 1797.
(26) Deffieux, A.; Schappacher, M. *Macromolecules* **2000**, *33*, 7371.
(27) Beers, K. L.; Gaynor, S. G.; Matyjaszewski, K.; Sheiko, S. S.; Möller, M. *Macromolecules* **1998**, *31*, 9413.
(28) Prokhorova, S. A.; Sheiko, S. S.; Möller, M.; Ahn, C.-H.; Percec, V. *Macromol. Rapid Commun.* **1998**, *19*, 359.
(29) Percec, V.; Ahn, C.-H.; Ungar, G.; Yeardley, D. J. P.; Möller, M.; Sheiko, S. S. *Nature (London)* **1998**, *391*, 161.
(30) Schlüter, A. D. *Top. Curr. Chem.* **1998**, *197*, 165.
(31) Förster, S.; Neubert, I.; Schlüter, A. D.; Lindner, P. *Macromolecules* **1999**, *32*, 4043.
(32) Stocker, W.; Schürmann, B. L.; Rabe, J. P.; Förster, S.; Lindner, P.; Neubert, I.; Schlüter, A.-D. *Adv. Mater.* **1998**, *10*, 793.
(33) Djalali, R.; Hugenberg, N.; Fischer, K.; Schmidt, M. *Macromol. Rapid Commun.* **1999**, *20*, 444.
(34) Börner, H. G.; Beers, K.; Matyjaszewski, K.; Sheiko, S. S.; Möller, M. *Macromolecules* **2001**, *34*, 4375.

(35) Cheng, G.; Böker, A.; Zhang, M.; Krausch, G.; Müller, A. H. E. *Macromolecules* **2001**, *34*, 6883.
(36) Rheingans, O.; Hugenberg, N.; Harris, J. R.; Fischer, K.; Maskos, M. *Macromolecules* **2000**, *13*, 4780.
(37) Zhong, Q.; Innis, D.; Eilings, V. B. *Surf. Sci. Lett.* **1993**, *290*, L688.
(38) Bantle, S.; Schmidt, M.; Burchard, W. *Macromolecules* **1982**, *15*, 1604.
(39) For the same reason GPC analysis was not successful. In THF the polymers did not elute, and in DMF/LiBr the elution peaks were seriously distorted most probably due to adsorption.
(40) Becker, A.; Köhler, W.; Müller, B. *Ber. Bunsen-Ges. Phys. Chem.* **1995**, *99*, 600.
(41) Gerle, M.; Fischer, K.; Schmidt, M. *Proc. ACS, Div. Mater.: Sci. Eng.* **1999**, *80*, 31.
(42) Fischer, K.; Schmidt, M. *Macromol. Rapid Commun.* **2001**, *22*, 789.

MA0113733